Original scientific paper

Informacije MIDEM
Journal of Microelectronics,
Electronic Components and Materials
Vol. 45, No. 4 (2015), 277 – 283

High-Efficiency Negative Charge-Pump Circuit for WLED Backlights

Yuwen Bao[1], XiaoLin Wu[2], Xiaohong Xia[1], Yun Gao[1]

[1]Faculty of Materials Science and Engineering, Hubei University, Wuhan, CO 430062, China
[2]Faculty of Physics and Electronic Technology, Hubei University, Wuhan, CO 430062, China

Abstract: Positive charge pumps, also known as inductor-less DC/DC converters, are very common in white LED drivers. They are less expensive and simpler to use, but they usually achieve a lower efficiency than inductor-based boost circuits. In this paper, we describe a novel negative charge-pump design for a white LED driver that can automatically select the 1X/1.5X mode. Unlike a conventional positive charge-pump circuit, the negative charge-pump circuit is integrated with current sources having an ultra-low dropout voltage, and the current source dropout is typically 80 mV. The negative charge-pump does not require an additional series-voltage-regulated transistor to adjust the output voltage, which can extend the operating time of the 1X mode and dramatically improve the efficiency of the lithium-ion battery. In addition, the negative charge pump does not require a substrate selection circuit, which reduces the circuit complexity. The proposed negative charge pump is realized in a 0.5-µm 5-V BiCMOS process.

Keywords: Current regulator; DC–DC power converters; LED driver; negative charge pump

Visoko učinkovito vezje negativne črpalke naboja za WLED osvetljevanje ozadja

Izvleček: Pozitivne črpalke naboja, ki jih poznamo kot DC/DC pretvornike brez tuljav, so zelo pogoste pri napajalnikih LED. So poceni in enostavne, vendar običajno dosegajo nižje izkoristke kot vezja na osnovi tuljav. V članku predstavljamo nov dizajn negativne črpalke naboja za napajanje belih LED, ki se avtomatsko postavijo v 1X/1.5X način delovanja. V nasprotju s pozitivnimi črpalkami naboja imajo negativne črpalke naboja integriran tokovni vir z izredno nizkim padcem napetosti (tipično 80 mV). Negativne črpalke naboja ne potrebujejo dodaten tranzistor za reguliranje izhodne napetosti, kar povečuje čas delovanja 1X načina in izboljša izkoristek litij-ionskih baterij. Predlagana črpalka naboja je realizirana v 0.5-µm 5-V BiCMOS tehnologiji.

Ključne besede: tokovni regulator; DC–DC močnostni pretvornik; LED krmilnik; negativna črpalka naboja

** Corresponding Author's e-mail: yungaoedu@126.com*

1 Introduction

The need for a white-LED (WLED) driver to illuminate the small color displays in cellular phones and other portable devices has increased rapidly over the last few years [1]. Currently, two approaches are commonly used to generate an adequate forward bias for WLEDs: a capacitor-charge pump and inductor-based boost circuits. Compared with inductor-based boost circuits, charge pumps are lower in cost, lower in working frequency, and simpler in design, but they have also been less efficient than inductor-based boost circuits [2]. However, efficiency might be the most important parameter for the designer of a portable device. Therefore, the improvement of the efficiency of charge-pump circuits becomes the key point of circuit design.

The operating voltage from most Lithium ion battery is 3 V to 4.2 V, while a WLED's forward voltage is typically 3.1 V to 3.5 V. Consequently, in order to improve the efficiency of the battery, an automatic-select multi-mode charge pump is used to provide an adequate forward bias for WLEDs. Presently a general choice is to use a two-mode (1X and 1.5X) charge pump [3–6]. A WLED is a current-driven device whose brightness is proportional to the conduction current. The conduction current is normally regulated to avoid exceeding the rated maximum current and to obtain a constant luminous intensity. As shown in Fig. 1, a traditional positive charge-pump solution for WLED drivers uses a PMOS regulator transistor to generate a regulated output voltage. The PMOS transistor before the charge-pump

stage is operated as a controlled resistance R_{DSON}, and regulation can be achieved by generating a voltage drop across R_{DSON}. The current regulator ensures that each WLED produces similar light output [7–9]. In Fig. 1, R_p is the parasitic resistance of the ground pad and bonding wire. Obviously, the key to improving the circuit efficiency focuses on lowering the voltage drop of the PMOS regulator transistor, R_p, and that of the current regulator.

To reduce the voltage drop of R_p and the current regulator, a current-regulated charge pump was designed for a WLED driver [10]. Fig. 2 shows the current-regulated charge pump scheme. The WLED can directly be connected to the system ground, and the current regulator transistor before the charge-pump stage is operated as a controlled current source I_{DS}. The current regulator transistor controls the pumping current, and output current regulation is accomplished by the changes in pumping current for all variations of the load [11]. The negative effect of R_p and the voltage drop of the current regulator are eliminated.

Parallel-connected WLED are commonly used in medium- and high-power driving WLED systems without the high cumulative voltage drop requirement, which is needed in series-connected driving WLED system. To cope with the current imbalance problem in parallel-connected WLED strings, a simple and highly efficient method is to have a current regulator for each WLED string [12]–[13]. However, the current-regulated charge pump (shown in Fig. 2) removes current regulator in order to obtain high efficiency, therefore it just suitable for driving a series-connected WLED string. If it is implemented in a 5 V process, it is only suitable for driving a single WLED. In practical applications, customers often need to drive multiple WLEDs and obtain high current matching accuracy.

This brief presents a novel negative charge pump for a plurality of driven WLEDs, as shown in Fig. 3. The scheme is composed of an automatic-select 1X/1.5X negative charge pump and a series current regulator. It is noted that there is no series voltage/current regulator transistor; therefore, the source–drain voltage drop of the regulator transistor can be saved, and high efficiency can be achieved. The anode of the WLED can be directly connected to the Li+ battery, and the cathode can be connected to negative charge pump. Hence, the current flowing through the WLED does not need to flow through the power pad of the chip, thereby removing the negative effect of the parasitic resistance of the power pad. In addition, the current regulator voltage dropout is typically 80 mV. All of these dramatically improve the efficiency, which allows the proposed negative charge pump to achieve the efficiency of inductor-based boost circuits.

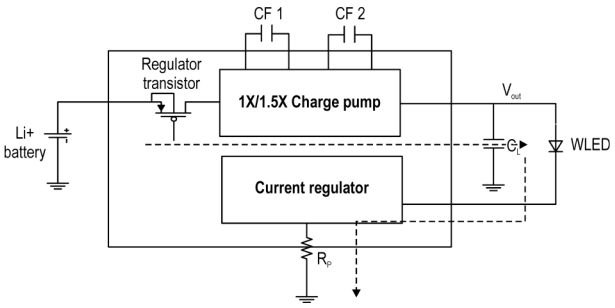

Figure 1: Conventional positive charge pump integrated with a constant current. The PMOS regulator transistor in the output loop operates as a controlled resistance and regulated output voltage.

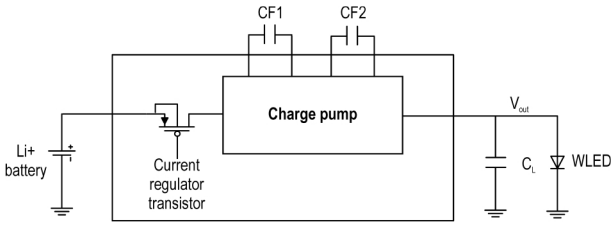

Figure 2: Current-mode charge pump that does not incorporate a series constant current. The pad parasitic resistance of the ground in the output loop is avoided.

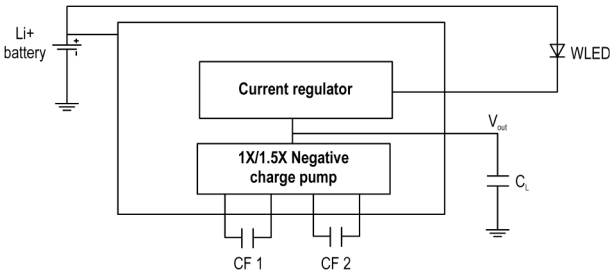

Figure 3: Proposed negative charge pump that does not incorporate a series regulator transistor. The pad parasitic resistance of the power source in the output loop is avoided.

Section 2 discusses the efficiency improvements of the negative charge pump, and Section 3 describes the 1X/1.5X negative charge-pump topology. Section 4 discusses the ultra-low dropout voltage of the current sources and the mode selection criteria. The experimental results are presented in Section 5, and the conclusions are drawn in Section 6.

2 Efficiency Improvements

Compared to an inductor-based boost DC/DC converter, a capacitor charge-pump converter is less efficient, which can reduce the battery runtime. A charge-pump scheme with an automatic-select conversion mode increases the efficiency over a wide input-voltage range. The quiescent operating current of the WLED driver is usually very small compared to the load current of the WLED; thus, the efficiency of fractional-ratio charge pumps with a conversion ratio of *M* can be closely approximated by

$$\eta = \frac{V_{LED}}{V_{IN} \times M} \tag{1}$$

where V_{IN} is the power source voltage, and V_{LED} is the voltage drop across the WLED. As can be deduced from (1), the efficiency versus V_{IN} will decrease as in the 1/x function for a fixed value of *M* [14], and the best conversion efficiency is offered by a 1X transfer mode (*M* = 1). However, this mode can only be used when the battery voltage is greater than the forward voltage of the WLED. It will be best for the driver to remain in a high-efficiency mode as long as possible while the battery voltage falls. Therefore, the main challenge in charge-pump design is to reduce the output-loop voltage losses. As shown in Fig. 1, the minimum battery voltage required by the 1X mode is:

$$V_{MIN(1X)} = I_{LED} \times R_{DSON} + V_{LED} + V_{Dropout} + I_{LED} \times R_p \tag{2}$$

where R_{DSON} is the source–drain conduction resistance of the regulator transistor, which is typically 2 Ω. Further resistance reductions are limited because lower resistances would necessitate a large MOS transistor, which increases the cost of the power device. $V_{Dropout}$ is the voltage dropout of the current regulator, which is about 250-300 mV [10]. The proposed circuit supports up to four white LEDs, and the maximum current for each WLED is about 20 mA, making I_{LED} 80 mA in total. V_{LED} of the WLED used for the simulation is 3.18 V, and R_p is ignored. The maximum efficiency of the 1X mode is 88.6%. The presented negative charge-pump topology does not require a regulated transistor, and it extends the 1X mode all the way down to

$$V_{MIN(1X)} = V_{LED} + V_{Dropout} \tag{3}$$

The designed current source dropout is typically 80 mV; therefore, the maximum efficiency of 1X mode can reach 97.5%.

3 Negative Charge-Pump Topology

Fig. 4 summarizes the topology transformations of the negative charge pump for the 1X and 1.5X modes. The double-modes negative charge pump includes six NMOS switches MN1-MN6、two PMOS switches MP1-MP2 and two flying capacitors CF1-CF2. By alternating the arrangement of switches and capacitors, it can realize two different conversion modes: 1.5X and 1X.

3.1 1.5X mode

During the first half period (0 to 0.5T), MOS switches MP1、MP2、MN4 are on, and the other MOS switches are off, CF1 and CF2 are in series connection and are charged by the power supply V_{IN}. The flying capacitors are equal to C, so the input voltage is evenly distributed across the two flying capacitors, and are charged to 1/2 V_{IN}.

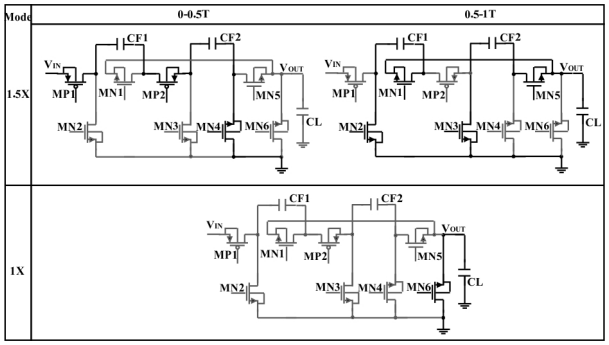

Figure 4: Topology transformations of the negative charge pump: 0–0.5T is the charge period for the flying capacitors, and 0.5–1T is discharge period

In the second half period (0.5T to T), the switches change their state, MOS switches MN1、MN2、MN3、MN5 are on and the other MOS switches are off. CF1 and CF2 are in parallel connection and one terminal is connected to ground, there is a charge redistribution between CF1、CF2 and CL. Assuming all the MOS switches are ideal. In a generic period *j* we get

$$V_{OUT}(\mathrm{j}) = V_{CL}(\mathrm{j}) = \frac{2C \times (-\frac{1}{2}\mathrm{V_{IN}}) + \mathrm{CL} \times \mathrm{V_{OUT}}(\mathrm{j}-1)}{2C + CL} \tag{4}$$

Assuming that in the initial state V_{OUT} (0) = 0 V, we get

$$V_{OUT} = -\frac{1}{2} V_{IN} \times (\frac{CL}{2C + CL})^j \tag{5}$$

whose limit for j →∞ is -1/2V_{IN}.

Indeed, the output voltage will steeply decrease and will slowly tend to its final value. The voltage between the input V_{IN} and the output V_{OUT} is 1.5V_{IN}.

3.2 1X mode

Only the MOS switch MN6 are always on, while the other switches are off, the output voltage V_{OUT} is connected to ground via the NMOS switch MN6, The voltage between the input V_{IN} and the output V_{OUT} is equal to V_{IN}. In the 1X mode the charge pump does not switch and act just like a LDO.

4 Current Source of the Ultra-Low Voltage Dropout and Mode Selection Criteria

4.1 Current Source of the Ultra-Low Voltage Dropout

The use of a current mirror is a common method for a current source. Fig. 5 presents a conventional current source for a WLED. The error amplifier guarantees that the current mirror (MN1 and MN2) source–drain voltages are approximately equal; the value of the WLED current is $260I_{ref}$ when the mirror ratio is 260. V_{OUT} is provided by the positive charge-pump output, and V_{ds} (MN2) is set to 250–300 mV in order to obtain high current matching accuracy. This increases the voltage consumption of the output loop and dramatically lowers the efficiency [10] [15].

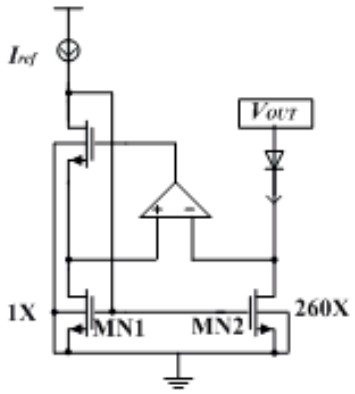

Figure 5: Conventional current source scheme.

Fig. 6 shows the scheme of the current source of the ultra-low voltage dropout and mode selection control circuit. The mirror transistor MN2 provides a constant current drain for the WLED, and V_{OUT} is the output of negative charge pump. It should be clear that source–drain voltage of MN2 is:

$$V_{ds2} = V_{IN} - V_{LED} - V_{OUT} \tag{6}$$

Thus, $V_{ds2} = V_{IN} - V_{LED}$ in 1X mode, and $V_{ds2} = 1.5V_{IN} - V_{LED}$ in 1.5X mode. The voltage of V_{ds2} is not a fixed value but rather a linear relationship with V_{IN}. Thus, MN2 provides not only the current source of the WLED but also acts as a regulator transistor, as shown in Fig. 1. The maximum current for each WLED is about 20 mA, which is much smaller than the total current; thus, further reducing V_{ds2} to 80 mV is feasible. In addition, the operating voltage range of the chip is 2.8–5 V, and V_{ds2} will be reduced to below 250 mV in a very small range of the operating voltage. Then, the slight decrease in the current matching accuracy in this range is acceptable.

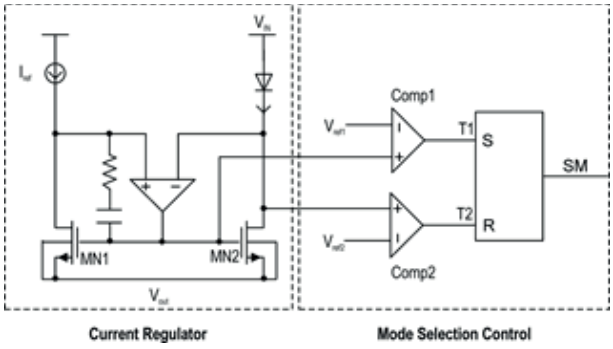

Figure 6: Current source of the ultra-low voltage dropout and mode selection control circuit.

4.2 Mode Selection Criteria

Fig. 6 also shows the mode selection control circuit that is used for the 1X/1.5X mode transition. Depending on the drop in the input voltage, the source–drain voltage (V_{ds2}) of MN2 decreases, and the gate–source voltage (V_{gs2}) of MN2 increases. V_{ds2} and V_{gs2} contain the real information of V_{IN} and the load. At $V_{ds2} \approx 80$mV, the circuit operating mode will change from the 1X mode to the 1.5X mode. MN2 operates in the linear region and $2(V_{gs2} - V_{th2}) >> V_{ds2}$. The current of the WLED is written as

$$I_{LED} = \mu_n C_{OX} \frac{W}{L}(V_{gs2} - V_{th2})V_{ds2} \tag{7}$$

Therefore, V_{ds2} is inversely proportional to V_{gs2}. In the design, we use V_{gs2} as the 1X to 1.5X mode transition as a control condition because V_{ds2} is very small at the point of the mode transition, and it is not suitable as the input voltage of Comp1. In addition, a small voltage change in V_{ds2} will cause a large voltage change in V_{gs2}. Therefore, the mode transition point from 1X to 1.5X can be accurately controlled.

A hysteresis voltage between the reference V_{ref1} and V_{ref2} is necessary to avoid uncontrolled toggling between the 1X mode and the 1.5X mode. Furthermore, V_{ref2} has to be larger than 80 mV to always guarantee stable DC operation in any mode. We set $V_{ref2} = 300$ mV; thus, the mode selection control circuits consist of Comp1 and

Comp2. The two comparators sense V_{ds2} and V_{gs2} and set or reset a flip-flop. The flip-flop stores the information of the mode change according to Table I.

Table 1: Mode Selection Depending on Comp1 Output T1 and Comp2 Output T2

Actual Mode	T1	T2	Set Mode
1X	H	L	1.5X
1.5X	L	H	1X

Fig. 7 shows the simulation results of the mode change due to a change in V_{IN}. The input voltage is swept from 5 V to 3.2 V and back to 5 V. When the input voltage drops, V_{ds2} drops below 80 mV (point A in Fig. 7), the Comp1 output T1 goes high, and the operation mode changes from 1X to 1.5X. When the input returns to the higher voltage, and V_{ds2} returns to 300 mV (point B in Fig. 7), the Comp2 output T2 goes high, and the operation mode returns to 1X. There is a hysteresis voltage of about 220 mV when transitioning from 1.5X to 1X.

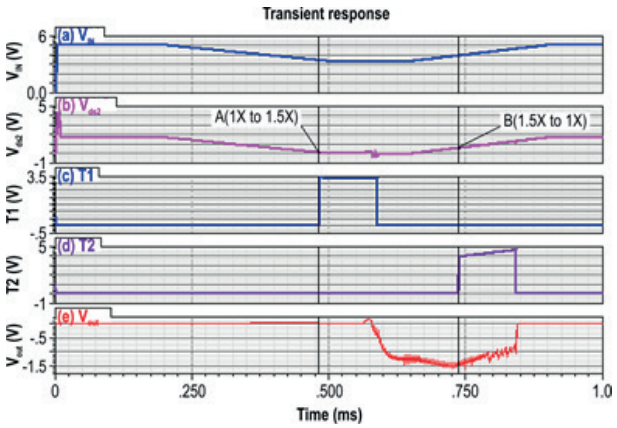

Figure 7: Effect of switching from the 1X mode to the 1.5X mode and back to the 1X mode on (a) the input voltage V_{IN}, (b) the source–drain voltage of MN2, V_{ds2}, (c) the Comp1 output T1, (d) the Comp2 output T2, and (e) the output voltage V_{OUT}. Point A indicates where V_{ds2} drops below 80 mV (transition from 1X to 1.5X). At point B, V_{ds2} returns to 300 mV (1.5X to 1X).

5 Experimental Results

The proposed circuit was implemented in a 0.5-um 5 V BiCMOS process by CSMC Technologies. For the simulation and experimental measurements, the external flying capacitors (CF1, CF2) and load capacitor (CL) are both 1 µF, V_{LED} of the WLED is 3.18 V when the WLED current is 20 mA, and the chip drives four WLEDs. Each LED current is set to approximately 20 mA.

The simulation and experimental measurement results in Fig. 8 show the efficiency versus the input voltage when the input voltage is swept from 5 V to 2.6 V. The results show that there is a sudden drop in efficiency at approximately 3.3 V. According to (1), we know that *M* of the charge pump has suddenly increased, and the negative charge pump switches from the 1X mode to the 1.5X mode at approximately 3.3 V. Further, the maximum efficiency from the simulation is approximately 93.2%. From Fig. 4, the 1X mode uses an NMOS (MN6) bypass switch to connect the output to the system ground. The parasitic resistance of MN6 will reduce the efficiency of the chip. This is the main reason why the maximum simulation efficiency is lower than the theoretical value. During the experimental measurement, the parasitic resistance of the pin pads and PCB routing and the ESR of external capacitors will further reduce the efficiency. In Fig. 7, the maximum measured efficiency is 89.3%, which is lower than that of simulation. Therefore, careful PCB routing is necessary to achieve the best performance.

The average measurement efficiency of the design over the entire input voltage range of a lithium-ion battery is approximately 75.2%. In contrast, an inductor-based boost circuit can achieve an efficiency between 75% and 80% [6]. Thus, our proposed scheme can achieve a high efficiency, as in an inductor-based boost scheme.

Fig. 9 shows measured currents of the four parallel WLEDs. When the chip operates in the 1X mode or 1.5X mode, the current of each WLED decreases as the input voltage decreases. In the operating voltage range (2.8–5 V), the current exhibits good stability, and the rate of change is less than 3.5%. There is always a gap between the four curves, and the maximum gap is about 0.4 mA (2%) due to the mismatch between the transistors of the current source for the WLEDs.

Fig. 10 shows the layout of the chip with a die size of 1.346 × 1.34 mm^2. The control and protect module comprises an oscillator operating at 250 kHz, a soft start function, an output over-voltage protection function, a 16-step brightness control function, an under-voltage lock-out function, and a mode change control.

6 Conclusion

Traditionally, WLED backlight designs that employ charge pumps have been less efficient than inductor-based designs. This brief has presented a negative charge pump with an ultra-low dropout current regulator. The novel negative charge architecture overcomes the inefficiencies typically encountered in a positive

charge pump, and it can achieve a peak efficiency of 89.3%. This negative charge pump is designed for use in WLED drivers, which enables a high efficiency to be realized while benefitting from the simplicity and cost savings offered by the charge-pump solution.

7 Acknowledgements

This work was supported in part by a Research and Development Grant from the Science and Technology Department of Hubei Province (Project ID: 2013BAA040, 2011BAB032).

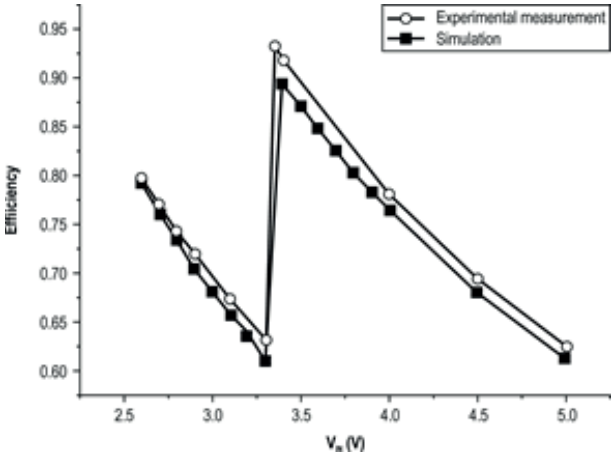

Figure 8: Simulated and measured efficiencies plotted as functions of the input voltage, swept from 5 V to 2.6 V. The sharp discontinuity at 3.3 V indicates the transition from the 1X mode to the 1.5X mode.

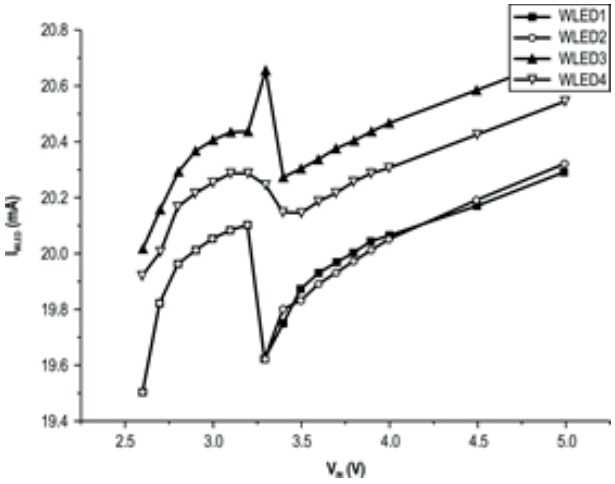

Figure 9: Measured currents of the four parallel WLEDs plotted as functions of the input voltage, swept from 5 V to 2.6 V. The charge rate of the WLED current is less than 3.5%, and the current mismatch is less than 2%.

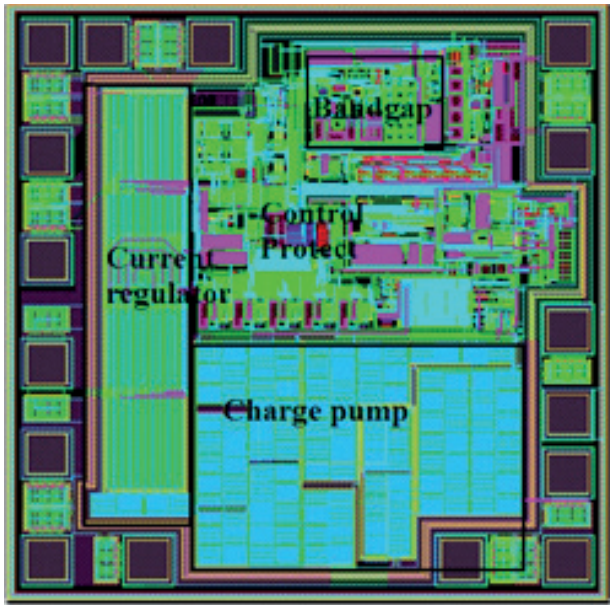

Figure 10: Layout of the proposed negative charge pump. The overall device dimensions are 1.346 × 1.34 mm^2.

8 References

1. R. Guo, Z. Liang, and A. Q. Huang, "A high efficiency transformerless step-up DC-DC converter with high voltage gain for LED backlighting applications," in *2011 Twenty-Sixth Annual IEEE Appl. Power Electron. Conf. Exposition*, Fort Worth, TX, 2011, pp. 1350–1356.
2. C. Richardson. (2007, Jan.). LED applications and driving techniques. National Semiconductor Corp., Santa Clara, California, USA. [Online]. Available:http://www.national.com/onlinesemimar/2007/led/national_LEDseminar.pdf
3. Q. Deng, "High efficiency multi-mode charge pump base LED driver," U.S. Patent 0109205, May. 25, 2006.
4. W.L. Deng, X.Y. Ma, W.Y. Huang, and J.K. Huang, "Design of a white LED backlight driver IC based on a new three-mode charge pump," in *2012 IET International Conf.*, Shenzhen, China, 2012, pp. 1–4.
5. Cao Y J, De H, Cao J M, et al. "High-Efficiency Charge Pump LED Driver Circuit Design," *Applied Mechanics and Materials,* vol. 389, pp. 612–617, Aug. 2013.
6. O. Nachbaur, "Leading light [portable device display illumination]" *Power Engineer*, vol. 19, no. 2, pp. 42–45, May 2005.
7. L. Burgyan and F. Prinz, "High efficiency LED driver," U.S. Patent 6690146, Feb. 10, 2004.

8. C.-H. Tsen, "Multi-mode charge pump drive circuit with improved input noise at a moment of mode change," U.S. Patent 7250810, Jun. 28, 2007.
9. T.-T. Chen and C.-H. Tsen, "Charge pump drive circuit for a light emitting diode" U.S. Patent 7271642, Sep. 18, 2007.
10. C.-H. Wu and C.L. Chen, "High-efficiency current-regulated charge pump for a white LED driver," *IEEE Trans. Circuits Syst. II, Exp. Briefs*, vol. 56, no. 10, pp. 763–767, Oct. 2009.
11. G. Thiele and E. Bayer, "Current mode charge pump: topology, modeling and control," in *2004 IEEE 35th Annual Power Electron. Specialists Conf.*, 2004, vol. 5, pp. 3812–3817.
12. Si Nan Li, Zhong W X, Chen W, Hui S S Y, "Novel Self-Configurable Current-Mirror Techniques for Reducing Current Imbalance in Parallel Light-Emitting Diode (LED) Strings," *IEEE Trans. Power Electronics*, vol. 27, no. 4, pp. 2153–2162, Apr. 2012.
13. Y. Hu and M. M. Jovanovic, "LED driver with self-adaptive drive voltage," *IEEE Trans. Power Electron.*, vol. 23, no. 6, pp. 3116–3125, Nov. 2008.
14. G. Thiele and E. Bayer, "Voltage doubler/tripler current-mode charge pump topology with simple "Gear Box"," in *2007 IEEE Power Electronics Specialists Conf.*, Orlando, FL, 2007, pp. 2348–2352
15. H. Van der Broeck, G. Sauerlander, and M. Wendt, "A high precision constant current source applied in LED driver," in *2011 Photonics and Optoelectronics. Conf.*, Wuhan, China, 2011, pp. 1–4.

Arrived: 06. 01. 2015
Accepted: 28. 10. 2015